Available online at www.sciencedirect.com
ScienceDirect
Journal of the European Ceramic Society 28 (2008) 41–48
www.elsevier.com/locate/jeurceramsoc

Thermoelectric ceramics for generators

J.G. Noudem *, S. Lemonnier, M. Prevel, E.S. Reddy, E. Guilmeau, C. Goupil

CRISMAT, CNRS/UMR 6508, ENSICAEN, 6 Bd Maréchal Juin, 14050 CAEN Cedex, France

Received 11 January 2007; received in revised form 25 April 2007; accepted 5 May 2007
Available online 6 August 2007

Abstract

The manufacturing of thermoelectric modules from conventional materials is well established and widely commercially available. However, fabrication of modules based on oxide materials has been recently emerging and there exist very few reports on their performance. The oxide nature of the thermoelectric elements and the processing specifications involving very high temperatures make the fabrication a difficult task and different from that of conventional thermoelectric modules. In this work we describe (i) the fabrication of thermoelectric modules based on oxide bulk and foam materials of $Ca_3Co_4O_9$ and $Ca_{0.95}Sm_{0.05}MnO_3$ and (ii) the metal to ceramic contact preparation. The open porous foam structures of thermoelectric materials make it possible to design efficient thermoelectric modules for waste heat sources involving gaseous and liquid media. The possibility of direct large area physical contact of thermoelectric foam elements with hot media will make them efficient electric power generators. The open porous thermoelectric materials with introduced porosities can be good candidates to confine phonons (lattice vibrations) in order to reduce the thermal conductivity if the pores can be made sufficiently small. The performances of the modules were evaluated and possible factors limiting their theoretical performance are discussed. A parameter representing the quality of the modules termed the manufacturing factor (MF) representing the cumulative effect of various factors involved in the fabrication process is introduced and evaluated for the modules and compared to other reported modules.

Keywords: Thermoelectric materials; Sintering; Ceramics

1. Introduction

Much effort[1–9] has been devoted to the development of manufacturing processes for oxide thermoelectric (TE) components with good performance in the last decade. These materials can directly convert heat into electricity (and vice versa). Thermoelectric energy conversion is achieved when a temperature difference is imposed externally across the TE-element. The early work on TE oxides was carried out in 1987.[1] This and other studies[2–12] have revealed the structure, magnetic and transport properties of the oxide compounds themselves. But to improve the thermoelectric properties and to define the design of the TE modules various studies were carried out.[13–16]

Oxide TE with large so-called figure of merit ZT is preferable. To be an effective thermoelectric material, a compound must possess a large Seebeck coefficient, a low resistivity and a low thermal conductivity. The oxide material must also be stable at high temperature and offer less toxicity compared to the intermetallic alloys $CoSb_3$, Bi_2Te_3, PbTe, etc. which easily decompose at high temperature and contains toxic heavy metals such as Hg, Te, Sb.

Scope of the present work is to deepen the understanding of contacts to TE at the level of their microstructure and to develop a robust technology for the preparation of low ohmic contacts to bulk TE oxides. In addition, the preparation of thermoelectric modules based on oxide bulk and foam materials of $Ca_3Co_4O_9$ and $Ca_{0.95}Sm_{0.05}MnO_3$ has been investigated. The open porous foam structures of thermoelectric materials have been processed and can result in efficient thermoelectric modules for waste heat sources involving gaseous and liquid media. The possibility of direct large area physical contact of thermoelectric foam elements with hot media will make them efficient electric power generators. The open porous thermoelectric materials with introduced porosities can be a good candidate to confine phonons (lattice vibrations) in order to reduce the thermal conductivity if the pores can be made sufficiently small.

* Corresponding author. Tel.: +33 231 45 13 66; fax: +33 231 95 16 00.
E-mail address: jacques.noudem@ensicaen.fr (J.G. Noudem).

0955-2219/$ – see front matter © 2007 Elsevier Ltd. All rights reserved.
doi:10.1016/j.jeurceramsoc.2007.05.012

Objectives of the present paper are:

- to prepare various forms of thermoelectric oxides using different process;
- to investigate the contact preparation and the correlation between apparent and effective contact area and to increase the effective contact area by using reactive solders;
- to introduce a manufacturing factor-MF considered from the thermal and electrical point of view and to compare the various oxide TE modules reported.

2. Experimental procedure

2.1. Material processing

2.1.1. p-Type and n-type bulks

Ceramic powders with nominal composition $Ca_3Co_4O_9$ namely 349 (p-type) and $Ca_{0.95}Sm_{0.05}MnO_3$ (n-type) were synthesized from stoichiometric amounts of $CaCO_3$, Co_3O_4, Sm_2O_3 and MnO_2 by "solid state reaction". The precursor powders were mixed and calcinated twice at 900 °C, for 12 h with intermediate grindings to obtain a homogeneous composition. The mixture powder is first formed into a cylindrical pellet (24 mm diameter) or bars (4 mm × 4 mm × 35 mm, Fig. 1) under 30 MPa using a compacting cell. According to the phase diagram,[17] the cobaltite samples were sintered in air at 920 °C, for 24 h. The polyvinyl alcohol was used as a binder in the case of the manganite compaction due to the coarser starting particle size. The processing temperature of the n-type material has been optimized as 1350 °C, 12 h. Beyond this temperature we observed that a few cracks started to appear along the bar samples. To overcome these problems, the temperature rate of 150 °C h^{-1} and dwell time of an hour at 1350 °C were optimized. In addition platinum plate used between the sample and Al_2O_3 crucible was crucial to prevent the reaction between the material and the support.

2.1.2. Porous n-type TE foams

The n-type thermoelectric $Ca_{0.95}Sm_{0.05}MnO_3$ (CSMO) foams of various porosities were produced as replicas of reticulated polyurethane foams. The use of polyurethane foams in processing of ceramic foam replicas is well known in the ceramic foam industry. Although the use of polyurethane foam is common for ceramic foam manufacturing, the actual fabrication process is specific to the composition of the material. The slurry for impregnation of polyurethane foams was prepared by mixing the ceramic powder in water with 5 wt.% polyvinyl alcohol as binder. The water content in the slurry is adjusted to be in the range of 20 wt.%. The choice of binders and plasticizers to result the required viscosity of the slurry and the thermal schedules for burning out of binders and sintering of the oxide material are important factors.

The CSMO powder used to prepare the slurries is processed by a standard solid-state preparation route from required amounts of high-purity, $CaCO_3$, Sm_2O_3 and Mn_2O_3. The stoichiometrically weighed powders were mixed in a ball mill for 2 h in ethanol followed by drying at ambient temperature. The dried powders in alumina crucibles were heated at a rate of 100 °C h^{-1} and fired for 24 h at 1050 °C. The annealed powders were further milled using zirconia balls to reduce the particle size to around a micron in agate ceramic pots placed on a centrifuge mill. The slurry for impregnation of the polyurethane foams was prepared by mixing the CSMO powder in water with 4 wt.% polyvinylalcohol as binder. It needs to be mentioned that the CSMO powder is chemically stable towards water allowing us to work with water-based slurries. The water content in the slurry is adjusted to be in the range of 20 wt.%. Commercially available polyurethane foams of 10 and 100 PPI (pores per inch) porosity were used to prepare thermoelectric oxide foams. The polyurethane foams were impregnated with thick oxide coatings by repeatedly dipping into the slurry with intermediate room temperature dryings. The dried foams with CSMO coatings were heated in a box type furnace in ambient atmosphere to burn out the polymer and further sintering of the oxide material. The binders and polyurethane are burnt by slow heating at a rate of 50 °C h^{-1} to 600 °C. A further heating to 1350 °C at 100 °C h^{-1} and dwelling for 24 h resulted in densification of the oxide powders into a structure replica of the foam.

2.2. Metal contacts to oxides

2.2.1. Preparation

It is well known[8,18,19] that good electrical contact preparation is essential for the design of thermoelectric (TE) modules for practical applications. Especially the resistance at contacts between TE and normal conductor has to be minimized. Simul-

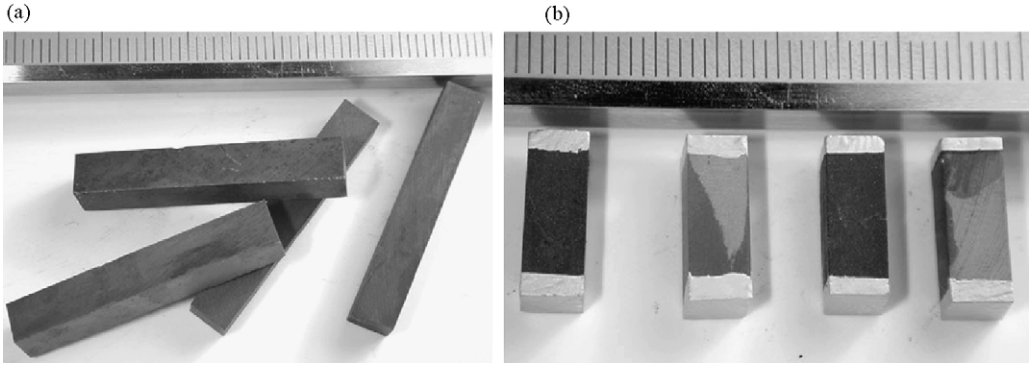

Fig. 1. (a) As-processed n- and p-type bar materials. (b) Ag–metal contacts processed for n and p type samples.

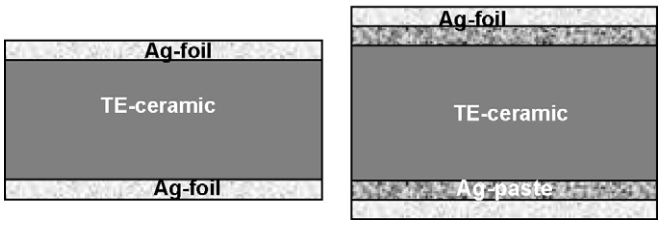

Fig. 2. Schematic diagram illustrating the contacts preparation.

taneously, the heat transfers across the interfaces need to be maximized.

Contacts were made to the TE (CaSmMnO) samples by the following two different methods:

(i) By painting the oxide material with commercial silver paste (silver conductor, 4929N, Dupont Inc. and 9912-A, ESL Inc.) using a brush and subsequent annealing at 900–935 °C for 1–5 h in order to metalize the paste and assist silver diffusion into the oxide ceramics. The difference between the silver paint is that ESL 9912-A contains fiber–glass inclusions to improve the mechanical strength of the contact.
(ii) In situ pressing silver sheet with TE oxide—in this method two possibilities have been investigated, silver metal foil (125 μm) has been connected directly to the TE pellet without any agent under 5 MPa stress. In addition, both commercial silver pastes mentioned earlier have been used at the interface between the TE oxide and silver foil. The main purpose of this additional coating is to increase the wettability at the interface during the process and also to promote possible silver diffusion into the ceramic. Moreover, the coating improves the adhesion between the Ag and TE material. Fig. 2 shows the schematic diagram of the configurations used for contacts preparation.

2.2.2. *Assembling TE oxides along with contact metals*

Practical applications of high temperature thermoelectric devices require certain length and/or complex shapes of the oxide elements. Different configurations have been investigated in this work:

(i) The in situ joining elements using silver foil. Basically, the silver plate of thickness around 1 mm seems to be necessary. The silver metal has been attached (Fig. 2) to the couple of sintered body of n-type $CaSmMnO_3$ and p-type $Ca_3Co_4O_9$ TE oxides with or without the commercial silver paste (4929N) followed by annealing at 900 °C for 5 h in order to improve the contacts.
(ii) Co-sintering or thermoforming using hot-pressing technique was also used for joining both n- and p-types materials (Fig. 3). This process yields stable modules similar to the design proposed by Shin et al.[16] The TE n-type sample previously sintered at (1350 °C, 12 h, air) was painted with Ag paste (Dupont 4929N) on both faces. The p-type pellets were placed between the two n-type samples and then joined by applying uniaxial pressure of 5 MPa. A processing temperature of 920 °C for 24 h in air was used to synthesize the 349 compounds. A slit of 1 mm was introduced between the n and p elements, as shown in Fig. 3, to result in a U-shaped structure. The motivation of this shaping is to prepare the long length module (e.g. zigzag shape, Fig. 3) where current could flow with a low resistance contact in order to improve the efficiency of the module.
(iii) Four leg TE modules with legs size of 10 mm were constructed. Fig. 4 shows a typical schematic diagram of a module. Basically, the modules were assembled using two pairs of p and n thermoelectric legs of 4 mm × 4 mm cross-section. The four thermoelectric elements are electrically connected in series by silver strips of 1 mm thick using silver paste as bonding agent. The assembly (Fig. 4) is placed between two alumina plates of 25 mm × 25 mm and 1.5 mm thick that stand thermally in parallel and act as hot and cold ends for thermoelectric legs. The assembled module is then subjected to a heat treatment at 915 °C for 5 h to metalize the silver paste at the junctions. This resulted in low ohmic and good thermal contacts and mechanical

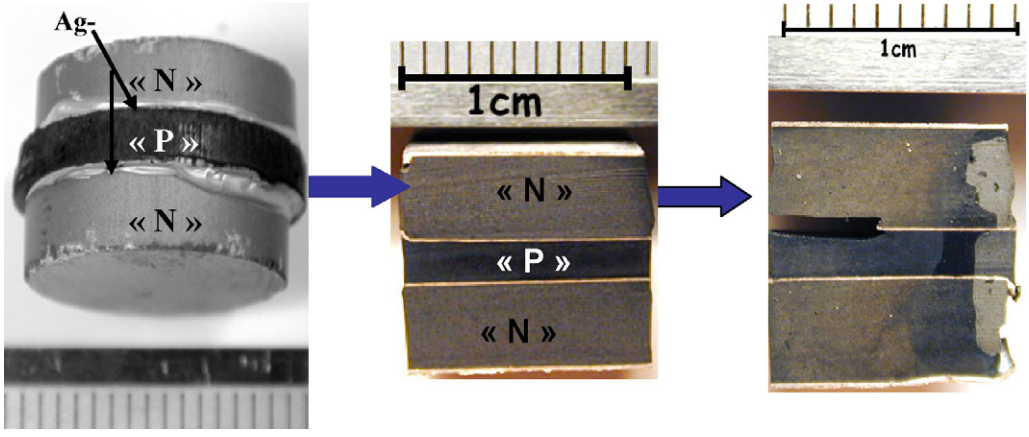

Fig. 3. Co-sintering of n-type/Ag-paste/p-type/Ag-paste/p-type and co-thermoforging, shaping Ag–metal/n-type/Ag-paste/p-type/Ag-paste/p-type/Ag–metal.

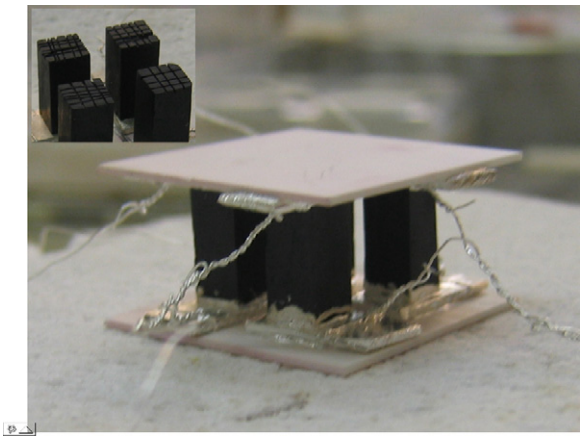

Fig. 4. Photograph showing a typical module fabricated using four n-type oxide legs (10 mm length). The mechanical and electric properties of the contacts were improved by increasing the surface area by grooving (figure in the inset) the ends of the oxide leg.

strength for the module. The details and arrangement used for measurements are described elsewhere.[13]

From the electrical point of view a thermoelectrical module is a voltage generator, it is completely described by its open voltage, E_0 and its internal resistance, R_{in}. In an ideal case E_0 is simply given by the sum of the Seebeck voltage contributions and the internal resistance, R_{in_ideal} as a lone contribution by the thermoelectric oxide material. However in practice, R_{in} is modified by the contact resistances leading to $R_{in} = R_{in\_ideal} + R_{contact}$. Maximum electrical output power can be extracted when the resistance load is equal to the internal resistance of the module $P_{max} = E_0^2/4R_{in}$. A simple "manufacturing factor" is estimated[20] by considering the ratio $MF = P_{max}/P_{max\_ideal}$.

3. Results and discussion

3.1. Contact characterization

After the contact preparation all samples were characterised by a standard dc four-probe method (Fig. 5) using PPMS (magnet power supply).

From the diagram of Fig. 5, the total electrical resistance of the bar sample is:

$$R_{tot} = 2R_c + 2R_1 + R_2, \quad \text{with } R_1 = \frac{\rho x L_1}{S}$$

where R_{tot} is the total resistance, R_c contact resistance, R_1 resistance between current and voltage taps, R_2 resistance between voltage taps, ρ sample resistivity, S sample cross-section and L_1 and L_2 are the lengths corresponding to R_1 and R_2, respectively.

On the other hand, the resistivity, ρ is an intrinsic parameter of the material and can be expressed as $\rho = R_2 x S/L_2$. The contact resistance is expressed in term of R_c

$$R_c = \frac{1}{2}x(R_{tot} - R_2) - \frac{2R_2 x L_1}{L_2}$$

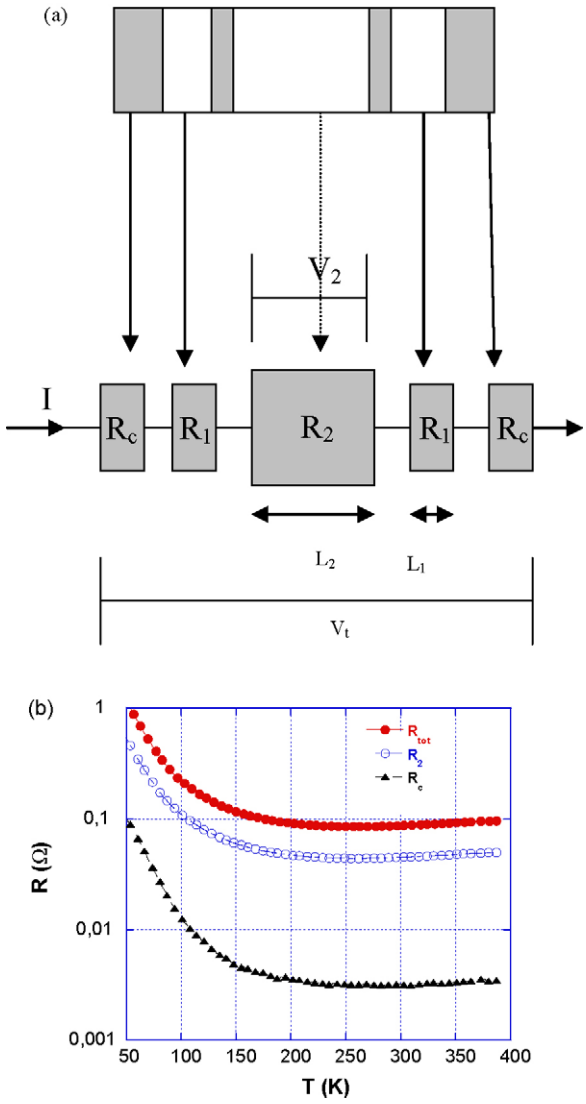

Fig. 5. (a) Block diagram showing the contact measurement schematics used to estimate the contact resistance, R_c. (b) Temperature dependence of the electrical resistance.

According to the following diagram (Fig. 5), where R_c is the contact resistance, R_2 the resistance of the material between voltage taps, R_1 the resistance between R_c and R_2 and the contact resistivity ρ_c is defined as $\rho_c = R_c x S$, where R_c is the contact resistance and S is the contact area. The room temperature resistivities of the contacts were found to be 290.41 and 1151 $\mu\Omega\,cm^2$ for the sample annealed with 9912-A and 4929N silver paste, respectively. The low ρ_c value can be related to the improvement of the contact due to the fibre–glass inclusions in the case of 9912-A. The in situ contacts processed under stress were also investigated. All ρ_c values among the various contact interfaces were found to be 12.70, 48.39 and 87.97 $\mu\Omega\,cm^2$ at 300 K for the TE/Ag foil, TE/Ag 9912A/Ag foil and TE/Ag 4929N/Ag foil, respectively. A possible explanation of the different contact values seems to be the effective contact area due to the diffusion of silver into the pores of TE material. Fig. 5b shows the typical electrical resistance as a function of temperature of the silver paste (4929N Dupont, Inc.) contact. One can observe that,

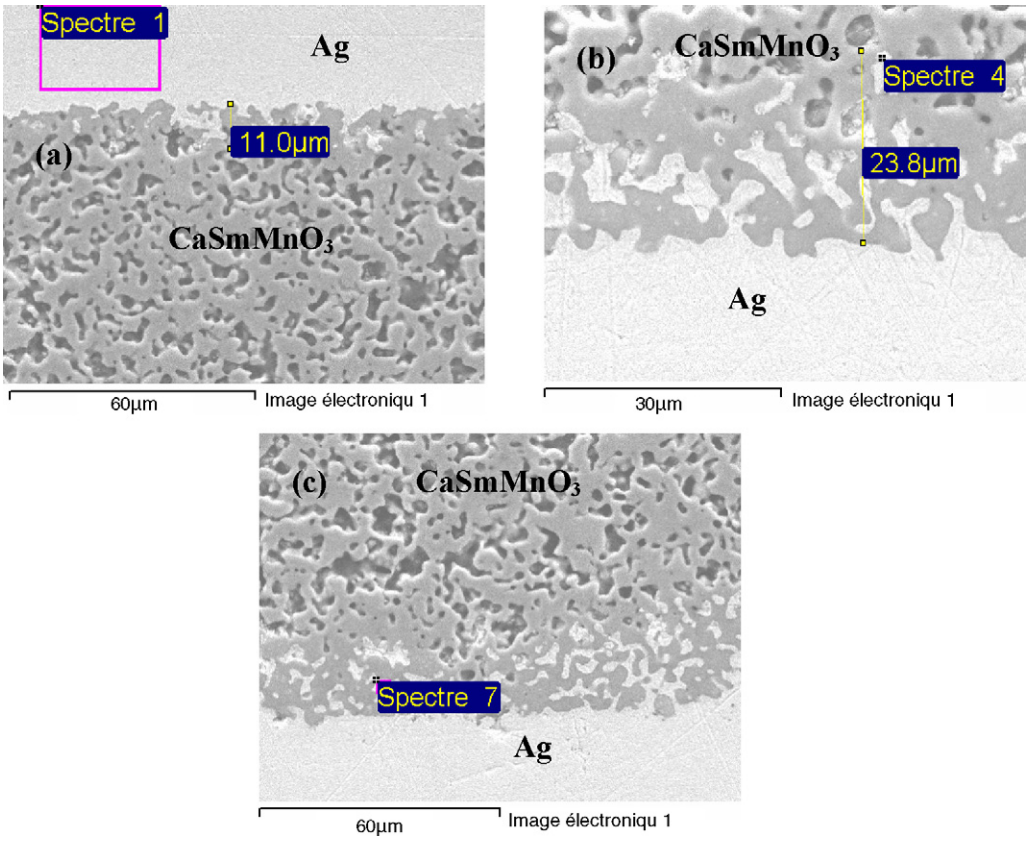

Fig. 6. Microstructures showing the flat interface between the Ag contact and $CaSmMnO_3$ ceramic. (a) TE/Ag foil, (b) TE/Ag 9912/Ag foil, (c) TE/Ag 4929/Ag foil. The flatness is probably due to the applied stress during the contacts processing.

the resistance decreases from low temperature to 200 K before becoming constant in all three cases.

Fig. 6 shows the microstructures of various interfaces for TE/Ag foil, TE/Ag 9912A/Ag foil and TE/Ag 4929N/Ag foil, respectively. One can observe that, all the interfaces seem to be planer. A good adherence can also be noticed. In the case where the silver paste has been used at the interface, silver is observed to infiltrate into the TE oxide up to 23 µm depth.

3.2. TE modules

The temperatures measured, reported elsewhere,[13] along a thermoelectric leg of hot and cold alumina plates show the proportionality of temperature gradients through the whole temperature range, indicating negligible radiation effects in the present module configuration. The electrical parameters of the module were extracted by repeating measurements in an open circuit and short circuit mode. The average Seebeck coefficients of the legs $\langle S \rangle$ were directly measured on the module, when working in an open circuit mode, while the resistivities, ρ, were extracted from the short circuit mode. All the physical parameters measured on the module are summarized in Table 1 and represent good agreement with the previous results reported for these thermoelectric oxides.[20,21] A power of 31.5 mW was obtained at a temperature of 750 °C. These values show that the oxides thermoelectrics, with their lightweight and high power densities are highly promising for generating electrical power at high temperatures.

In this study, it needs to be highlighted that a good manufacturing factor of 59% has been obtained without using a modified silver paste for the contacts preparation or going for uniaxial pressure during manufacturing or measurements as previously reported.[8] The manufacturing factor of 59% indicates the possibility of obtaining high quality modules with the present design and manufacturing method. When compared to the current status of oxide modules, a highest manufacturing factor of 86% could be estimated from the reported[8] values for a CaBiCoO/LaBiNiO couple prepared and measured under uniaxial pressure. It may

Table 1
Physical parameters measured for the four legs thermoelectric

T_{hot} (K)	990
ΔT (K)	630
$\langle S_p \rangle$ (µV K^{-1})	145
$\langle S_n \rangle$ (µV K^{-1})	−178
ρ_n (mΩ cm)	10
ρ_p (mΩ cm)	50
E_0 (mV)	400
R_{in_ideal} (Ω)	0.75
R_{in} (Ω)	1.27
$R_{contact}$ (Ω)	0.52
P_{max_ideal} (mW)	53
P_{max} (mW)	31.5
Manufacturing factor μ (%)	59

be noticed that the manufacturing factor values obtained on the present module result without using any applied pressure and also measured in ambient pressure. The present value is also higher then that of the modules prepared with optimized quality of contacts by using a mixture of silver paste and corresponding oxide powder reported elsewhere.[8]

Manufacturing process is the dominating factor deciding the efficiency of the modules. For commercial modules usually MF values in the range of 60–80% were reported.[22] The thermal contacts are due to the interface of the oxide legs with the top and bottom insulating plates. Improving this interface i.e., the mechanical integrity of the module, particularly at high temperatures, by using oxide legs of uniform thermal expansion coefficients is an important factor in improving the efficiency of the module. It is also worth noticing that poor electrical contacts quality will also strongly reduce the output power of the modules.

The high manufacturing factor obtained in the present case, without using any modified silver paste or going for uniaxial pressure during manufacturing, could be explained as due to the modifying of the effective contact resistance. The grooves made on the oxide materials (inset Fig. 4) before contact preparation probably improve the contact resistivities as reported for the cuprate superconductors.[23] The possibility of using high metallization temperatures for Ag paste, close to the melting point of Ag, due to the choice of high melting oxide elements has also played an important role in improving the manufacturing factor due to the improved electric contacts.

3.3. TE foams characterization

Fig. 7 shows the macrographs of as-processed thermoelectric foams of different porosities. The thickness of the struts is calculated to be less than 100 μm and the relative density is around 20% in case of 100 PPI porosity foam with respect to its bulk counter part. The fractured surface of the foams, Fig. 8, reveals dense microstructure of the struts with average grain size of 3 μm. The X-ray diffraction pattern of the powdered foam taken with Cu Kα radiation is shown in Fig. 8b. All peaks were indexed for $Ca_{0.95}Sm_{0.05}MnO_3$ phase with no presence of impurities. The EDAX chemical analysis also indicated no traces of carbon residue from the organics used for preparation.

The ability of the oxide foam structures as thermoelectric generators is demonstrated in a simple configuration as shown schematically in Fig. 9. A 100 PPI foam of 30 mm × 10 mm × 10 mm was used for the experiment. The electrical contacts for the oxide foams were made by coating silver paint up to around 2 mm length, Fig. 9b, on both ends and metalizing at 935 °C for 5 h. The performance is evaluated by heating one end of the foam by a butane + propane flame torch and simultaneously recording various parameters, viz., temperatures along the length of the foam, open circuit current and voltage, internal resistance and Seebeck coefficients by an automated Keithley K2700/7700 scanning system and a computer. Temperature gradients of around 500 °C were created along the length of the thermoelectric foam by heating one end of the foam to 575 °C and placing the other end in ambient air. The temperatures recorded, by three *k* thermocouples, along the length of the foam in a typical run is shown in Fig. 10. The Seebeck coefficient directly measured on the foam, when working in an open circuit mode, is shown as inset in Fig. 10. The various parameters recorded are summarized in Table 2. An open circuit voltage of 100 mV was generated at an operation temperature of 575 °C with 500 °C gradient and internal resistance of 12 Ω. A maximum output power of 1 mW was obtained.

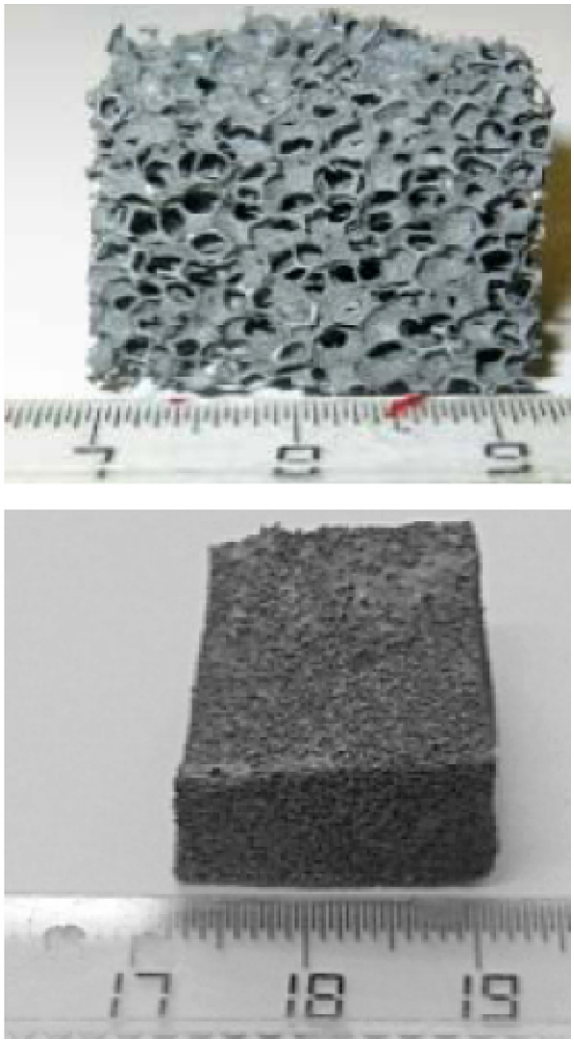

Fig. 7. As-processed thermoelectric $Ca_{0.95}Sm_{0.05}MnO_3$ open porous replica of polyurethane foams with porosities of (a) 40 PPI and (b) 100 PPI.

The outlook for oxide foam structures is quite promising. The availability of thermoelectric foams could result in designing of unique and efficient thermoelectric modules for specific heat source environments. The oxide thermoelectric foams are also

Table 2
Physical parameters measured for the foam thermoelectric

T_{hot} (K)	575
ΔT (K)	500
$\langle S_p \rangle$ (μV K^{-1})	−197
R (Ω)	12.5
E_0 (mV)	100
P_{max} (mW)	1

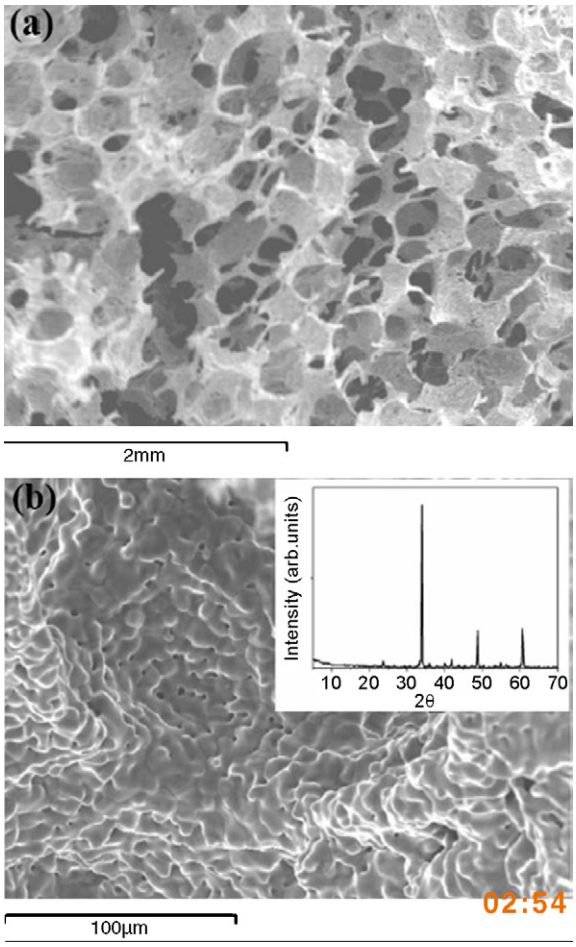

Fig. 8. (a) SEM microstructure of a fractured surface of 100 PPI thermoelectric foam. The dense structure of the struts can be noticed in figure (b). The inset shows the XRD pattern of the powdered $Ca_{0.95}Sm_{0.05}MnO_3$ foam.

of interest to replace the bulk thermoelectric elements in the conventional module designs. Basically, the efficiency of the thermoelectric materials is interplay between the electrical and thermal conductivities. The dimensionless efficiency factor is given by $ZT = S^2\sigma/\kappa$, where S is the Seebeck coefficient and σ and κ are the electrical and thermal conductivities, respectively.

Foams are well known to have very different effective properties as compared to the bulk counterparts.[24,25] At high porosities, exceeding 90%, various theoretical models,[24,25] indicate that the effective rate of increase in electrical conductivity is more than

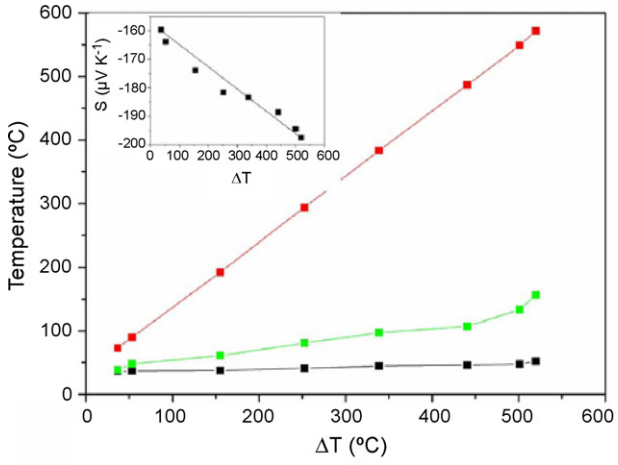

Fig. 10. The measured temperatures along the length of the foam. The inset shows the Seebeck coefficient of the foam. The fluctuations in the values are due to the inability to maintain precise temperature stability along the length of the foam due to the nature of the heat source, flame torch used.

that of thermal conductivity. Finding an optimal porosity with increased ratio of the electrical to thermal conductivities for a given thermoelectric foam element could result in increasing the ZT and hence the efficiency of the thermoelectric generator. Another advantage of the foam structure being that the large surface area of foams could result in fabricating low ohmic electrical contacts to the thermoelectric materials.

4. Conclusion

In this paper, we have reviewed our current work on thermoelectric oxides forming, contact resistance preparation, module manufacturing and characterization. We demonstrated the different ways to prepare and improve the contact resistivities, connection (metal contacts to oxides) between p-type and n-type and finally the feasibility to design the TE module.

The manufacturing of foams from oxide thermoelectric materials and the concept of using foam structures for waste heats involving gaseous and liquid environments have been discussed. The high surface area of the foams allows an efficient heat extraction as compared to the bulk materials. The thermoelectric $Ca_{0.95}Sm_{0.05}MnO_3$ material has been processed as replica of polyurethane foams and demonstrated to be a thermoelectric generator.

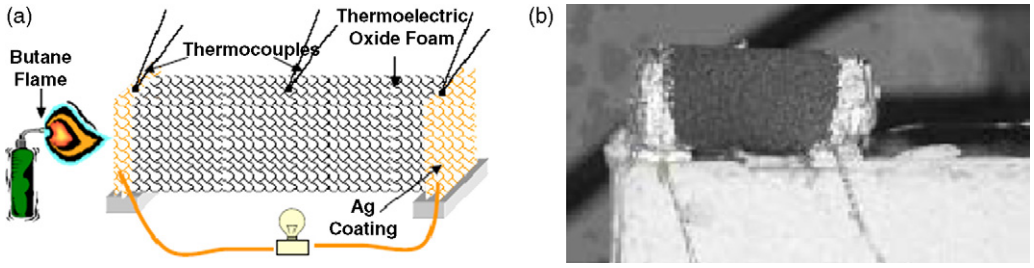

Fig. 9. (a) Schematic diagram illustrating the configuration used to evaluate the thermoelectric foam as a thermoelectric generator. The heat source used is a butane + propane flame torch. (b) The inset shows a 100 PPI $Ca_{0.95}Sm_{0.05}MnO_3$ foam fabricated accordingly. The electrical contacts, at the ends of the foam, are fabricated by painting silver paste and metalizing at 935 °C.

The thermoelectric properties and performances of the modules were evaluated and possible factors limiting their ideal performance are discussed. A parameter representing the quality of the modules termed as manufacturing factor (MF) representing the cumulative effect of various factors involved in the fabrication process was introduced and evaluated for the modules and compared to other reported modules.

Acknowledgments

The authors wish to acknowledge the financial support from Conseil Régional de Basse Normandie, France. S. Lemonnier and M. Prevel are grateful to the "French Ministère de la Recherche et de la Technologie" for their Ph.D. fellowship.

References

1. Terasaki, I., Sasago, Y. and Uchinokura, K., *Phys. Rev. B*, 1997, **56**, R12685.
2. Hervieu, M., Boullay, Ph., Michel, C., Maignan, A. and Raveau, B., *J. Solid State Chem.*, 1999, **142**, 305.
3. Masset, A. C., Michel, C., Maignan, A., Hervieu, M., Toulemonde, O., Studer, F., Raveau, B. and Hejtmanek, J., *Phys. Rev. B*, 2000, **62**, 166.
4. Yamamoto, T., Tsukada, I., Uchinokura, K., Takagi, M., Tsubone, T., Ichihara, M. and Kobayashi, K., *Jpn. J. Appl. Phys.*, 2000, **39**, 747.
5. Masuda, Y., Nagahama, D., Itahara, H., Tani, T., Seo, W. S. and Koumoto, K., *J. Mater. Chem.*, 2003, **13**, 1094.
6. Xu, G., Funahashi, R., Shikano, M., Matsubara, I. and Zhou, Y., *J. Appl. Phys.*, 2002, **91**, 4344.
7. Funahashi, R. and Urata, S., *J. Mater. Res.*, 2003, **18**, 1646.
8. Funahashi, R., Urata, S., Mizuno, K., Kouuchi, T. and Mikami, K., *Appl. Phys. Lett.*, 2004, **85**, 1036.
9. Prevel, M., Lemonnier, S., Hébert, S., Chateigner, D., Ouladdiaf, B., Klein, Y. and Noudem, J. G., *J. Appl. Phys.*, 2005, **98**, 093706.
10. Klein, Y., Pelloquin, D., Hébert, S., Maignan, A. and Hejtmanet, J., *J. Appl. Phys.*, 2005, **98**, 13701.
11. Maignan, A., Flahaut, D. and Hébert, S., *Eur. Phys. J.*, 2004, **B39**, 145.
12. Grebille, D., Lambert, S., Bouiee, F. and Petricek, V., *J. Appl. Crystallogr.*, 2004, **37**, 823.
13. Sudhakar Reddy, E., Noudem, J. G., Hebert, S. and Goupil, C., *J. Phys. D: Appl. Phys.*, 2005, **38**, 3751.
14. Funahashi, R., Mikami, M., Mihara, T., Urata, S. and Ando, N., *J. Appl. Phys.*, 2006, **99**, 066117.
15. Matsubara, I., Funahashi, R., Takeuchi, T. and Sodeoka, S., *J. Appl. Phys.*, 2001, **90**, 462.
16. Shin, W., Murayama, N., Ikeda, K. and Sago, S., *Jpn. J. Appl. Phys.*, 2000, **39**, 1254.
17. Woermann, E. and Muan, A., *J. Inorg. Nucl. Chem.*, 1970, **32**, 1455.
18. Caillat, T., Fleurial, J.P., Snyder, G., Zoltan, G.J., Zoltan, D. and Borshchevsky, A., Proceeding of the 18th International Conference on Thermoelectrics, Proceeding of the XVII International Conference on Thermoelectrics, Baltimore, USA, IEEE Catalog Number 99TH8407, 473, 1999.
19. Caillat, T., Fleurial, J.P., Snyder, G., Zoltan, G.J., Zoltan, D. and Borshchevsky, A., Proceedings of the 34th Intersociety Energy Conversion Engineering Conference 2567, 1999.
20. Suzuki, K., Fujishiro, H., Kashiwada, Y., Fujine, Y. and Ikebe, M., *Phys. B*, 2003, **329–333**, 922.
21. Miyazaki, Y., *Solid State Ion*, 2004, **172**, 463.
22. Rowe, D. and Min, G., *J. Power Sources*, 1998, **73**, 193.
23. Noudem, J.G., Tarka, M. and Schmitz, G.J., Inst. Phys. Conf. Ser. No. 167, EUCAS, 14–17 September, Spain, 183, 1999.
24. Dharmasena, K. P. and Wadley, H. N. G., *J. Mater. Res.*, 2002, **17**, 625.
25. Langlois, S. and Coeuret, F., *J. Appl. Electrochem.*, 1989, **19**, 43.